3D wave equation migration improves prospectivity by enhancing subsalt imaging

Nanxun Dai, Chris N. Willacy, Ruben V. Pascual, Lawrence M. Gochioco, Yong Sun, and Brent B. Mecham, GX Technology, Houston, Texas, U.S.

The convergence of advanced computing technologies and innovative algorithm designs has made it possible to provide 3D Wave Equation depth migration methods to many explorationists. It is well known that the wave equation method can provide the full wavefield solution to most imaging problems, when compared to the Kirchhoff technique, which has become the industry's standard prestack depth migration (preSDM) algorithm. Even though various implementation techniques have expanded its capabilities, notably with respect to traveltime estimation, the Kirchhoff method has some inherent limitations, such as diverging ray paths in steeply-dipping areas were high lateral velocity contrasts exist. More accurate imaging in such challenging geologic conditions can often be addressed by a Wave Equation (W.E.) depth migration solution. Dramatic reductions in computing costs have facilitated the gradual employment of the W.E. migration method.

Numerous examples have been presented by other investigators comparing the results of the two methodologies, as applied to the 3D SEG/EAGE salt model. This paper however, presents results from a case study conducted on the US Gulf Coast where the 3D Kirchhoff preSDM method was initially used to enhance the images of a salt body and surrounding sediments. This was followed by the application of the W.E. migration solution to yield finer details of the subsurface, especially subsalt structure.

The wave equation method used in this study is a shot-based approach that employs the phase-shift and split-step Fourier plus interpolation (SSFPI) algorithms for wavefield downward extrapolation. These two approaches are adaptively implemented according to the velocity model structure. Phase shift is used in constant velocity areas (water column, salt bodies), while SSFPI is used in sedimentary strata with varying velocity. The separation of salt (including water in offshore areas) from the sedimentary background greatly reduces the number of reference velocities required in the SSFPI algorithm. In comparison to other extrapolation methods such as the Fourier finite difference (FFD) algorithm, phase-shift and SSFPI do not suffer from numerical dispersion or anisotropy problems and are accurate at wide angles. High angle imaging is further improved by employing a modified imaging condition that compensates uneven energy distribution due to velocity variation and oblique factors in the extrapolated wavefield; thus, providing enhanced amplitudes for steeply dipping events.

The prospect area, which has been producing oil and gas for decades, is located along the US Gulf Coast. A gravity survey initially detected the onshore salt body, and indicated that the salt was probably a hanging structure and not rooted to the basement. Two-dimensional (2D) seismic surveys followed and the data provided more subsurface information. Based on these two different geophysical data sets, wells were drilled, and oil and gas producing sands were discovered from depths ranging from 3,000 to 10,000 feet beneath the surface.

Additional geologic information provided by well logs and production data indicate that there is still a considerable amount of hydrocarbons to be discovered. Increasing hydrocarbon production is a viable option, only if the salt body and subsalt structures can be accurately mapped. In addition, knowing the extent and delineation of faults emanating from the salt body is important because it can provide a better understanding of the migration and trapping mechanisms for the hydrocarbons. Thus, a three-dimensional (3D) seismic survey was subsequently conducted to assist interpreters to better map the boundary of the salt body and its associated faults, and to therefore better determine future well locations.

Figure 1 shows the field layout of the 3D seismic survey conducted over the salt structure. The study area covers approximately 51 square miles. Receivers were planted in a southwest-to-northeast direction, and the sources were shot orthogonal to the receiver layout in a brick pattern. The maximum offset was 18,000 feet. Surface topography is relatively flat, with elevations between 0 and 2 feet above sea level. Following the acquisition and time processing, a prestack time migration was run. This however, did not sufficiently image the base salt and subsalt structures. Prestack depth migration and velocity model building was finally used to try to improve the imaging.

The 3D prestack time migration (preSTM) section of a crossline, located near the center of the survey area is shown in Figure 2. The time section shows relatively good top-of-salt and suprasalt sediment images and shows the salt as a triangular-shaped body. Dead traces observed on the left-hand side of the figure correspond to areas which were not acquired due to permitting problems. As illustrated in the figure, the subsalt reflections are poorly focused and not correctly positioned spatially by the preSTM.

In comparison, the Kirchhoff preSDM image of the same crossline, presented in Figure 3, shows improvements in the suprasalt sediments, as well as better focusing of the steep salt flanks. The depth section ranges from 60 to 19,850 feet. Significant improvements are evident in the imaging of the base of salt and some subsalt structures are interpretable. With the base of salt imaged, Figure 3 clearly shows the outline of a diamond-shaped salt body with some underlying structures. The W.E. method was also employed and the resulting image is shown in Figure 4. The salt flanks exhibit a small improvement compared to the Kirchhoff image. However, the W.E. section shows much improved subsalt reflections at about 17,000 feet depth, as indicated in Figure 4.

When examining the Kirchhoff and W.E. images of the hanging salt structure, it becomes apparent that the W.E. image exhibits a lower frequency spectrum. This resulted from attempts to save on processing cost by tapering the high frequency range to between 30- and 35-Hz, while the spectrum of the Kirchhoff image was kept open up to between 60- and 65-Hz. No shot decimation was applied in the wave equation processing.

Even though the higher frequencies in the W.E. image were filtered to save on computing time and costs, image quality was not compromised. To support this analysis, we present a different perspective view, such as looking at a depth slice display. Depth slices of the Kirchhoff and W.E. 3D data volume at 4980 feet are presented in Figures 5 and 6, where the focus is on the definition of suprasalt sediments and fault definition. The arrows in each figure highlight what we believe are better-imaged faults. Thus at this depth level, the Kirchhoff and W.E. methods yielded comparable results, with no solution distinctly outperforming the other.

In the subsalt environment, however, the Kirchhoff technique is often plagued by artifacts that develop when the theoretical limits of the method are reached. Irregularly-shaped structures such as this salt geometry cause the raypaths to diverge. Such scattering of the wavefield produces low subsalt fold coverage, and hence, lower amplitudes and an overall defocused or shadow zone. Figure 7 shows the Kirchhoff preSDM of an inline section, highlighting the subsalt depth interval of between 11,900 and 25,500 feet. A moderate outline of the base-of-salt is evident at a depth of about 13,600 feet. The two arrows indicate an interval of weak subsalt structural imaging. The weak and discontinuous structures might suggest some type of faulting – a risky misinterpretation. In contrast, the W.E. preSDM image, displays a more enhanced image of the subsalt structure, as indicated in Figure 8. It is apparent that there is structure beneath the salt body forming a rollover or structural high.

Another example is presented in Figure 9, where the Kirchhoff preSDM image of a crossline shows a very good image of the base salt. It is quite interpretable to see where the sediments truncate against the salt body and near the base-of-salt. As expected, subsalt imaging via the Kirchhoff method is rather poor and the discontinuous structures could be misinterpreted as faults. On the other hand, the W.E. preSDM image in Figure 10 shows not only a good base-of-salt image, but also better defined subsalt reflections. The more enhanced subsalt images provided by the W.E. solution will certainly increase the value and prospectivity of this property.

In summary, the Kirchhoff preSDM method will continue to be the preferred choice for prestack depth imaging projects because it is computationally more efficient than the wave equation method. Depending on the type of implementation, the Kirchhoff method can achieve solutions with accuracy. However, it is important to understand its capabilities and limitations. On the other hand, we view the wave equation method, not as a replacement, but as a complementary technology to Kirchhoff, whereby it can be used in certain conditions to enhance imaging of subsurface structures. As was demonstrated in this paper, the wave equation method did enhance subsalt structures, potentially adding more value to the prospect. Cost is a major factor that currently inhibits greater employment of the wave equation solution. But, as we have witnessed in recent years, it is just a matter of time before improved implementations of the 3D wave equation method will make it more efficient and price competitive.

Acknowledgement. The authors thank Burlington Resources for permission to use their data and GXT for permission to publish this paper.

Suggested Readings. "Anti-aliasing methods in Kirchhoff migration" by Abma et. al. (Geophysics, 1999), "Wave equation migration with the phase-shift method" by Gazdag (Geophysics 1978), "Migration of seismic data by the phase-shift method" by Gazdag and Sguazzero (Geophysics 1984), "True amplitude seismic migration: A comparison of three approaches" by Gray (Geophysics 1997), "Depth imaging of Gulf Coast salt dome" by Pascual et. al. (American Oil & Gas, 2001), "Fourier finite difference migration" by Ristow and Rhul (Geophysics 1994), "Split-step Fourier migration" by Stoffa et. al. (Geophysics 1990) and "Steep dip imaging with wave equation prestack depth migration" by Dai et al. (CSEG Abstracts 2002).

Corresponding author: nxd@gxt.com

List of Figure Captions

Figure 1. Map of study area showing the layout of the survey grid.

Figure 2. Pre-stack time migration section of a crossline located near the center of the survey area.

Figure 3. Kirchhoff preSDM section of the crossline in Figure 2.

Figure 4. Wave Equation preSDM section of the crossline in Figure 2.

Figure 5. Depth slice (at 4980 ft) of the 3D Kirchhoff preSDM volume.

Figure 6. Depth slice (at 4980 ft) of the 3D Wave Equation preSDM volume.

Figure 7. Kirchhoff preSDM image of subsalt structures from an inline.

Figure 8. Wave Equation preSDM image of the same inline in Figure 7, highlighting subsalt structures.

Figure 9. Kirchhoff preSDM image of subsalt structures from a crossline.

Figure 10. Wave Equation preSDM image of the same crossline in Figure 9, highlighting subsalt structures.

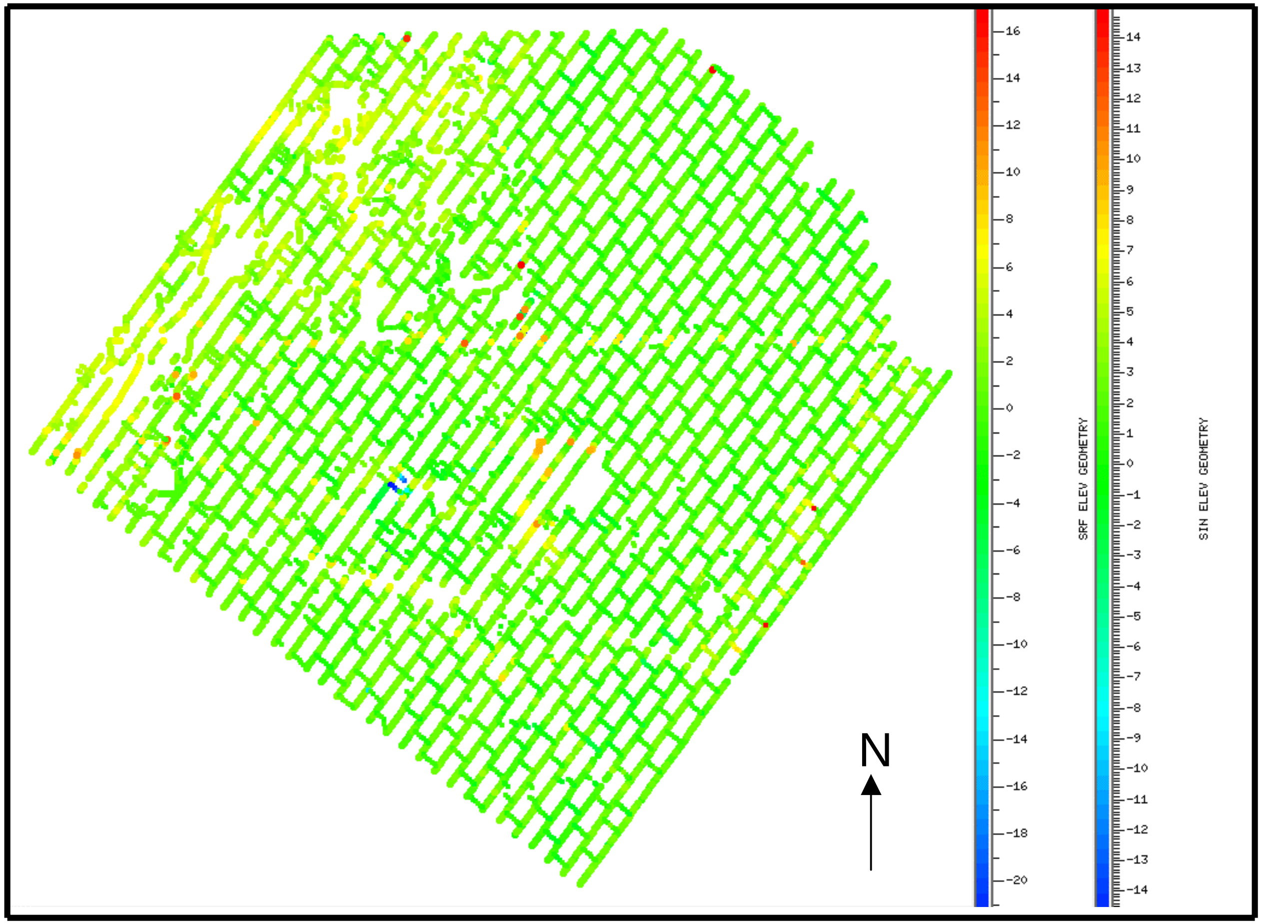

Figure 1.

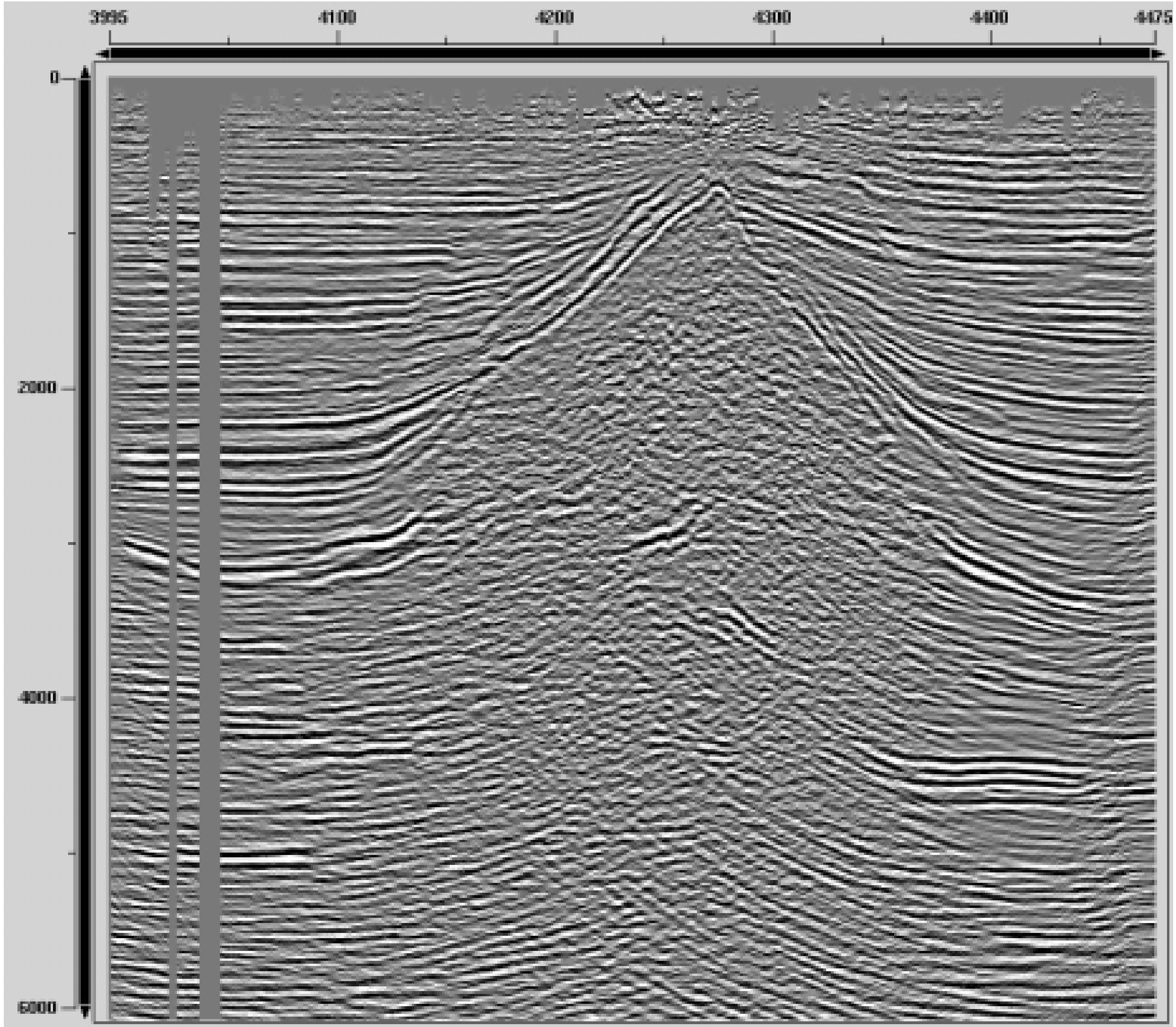

Figure 2.

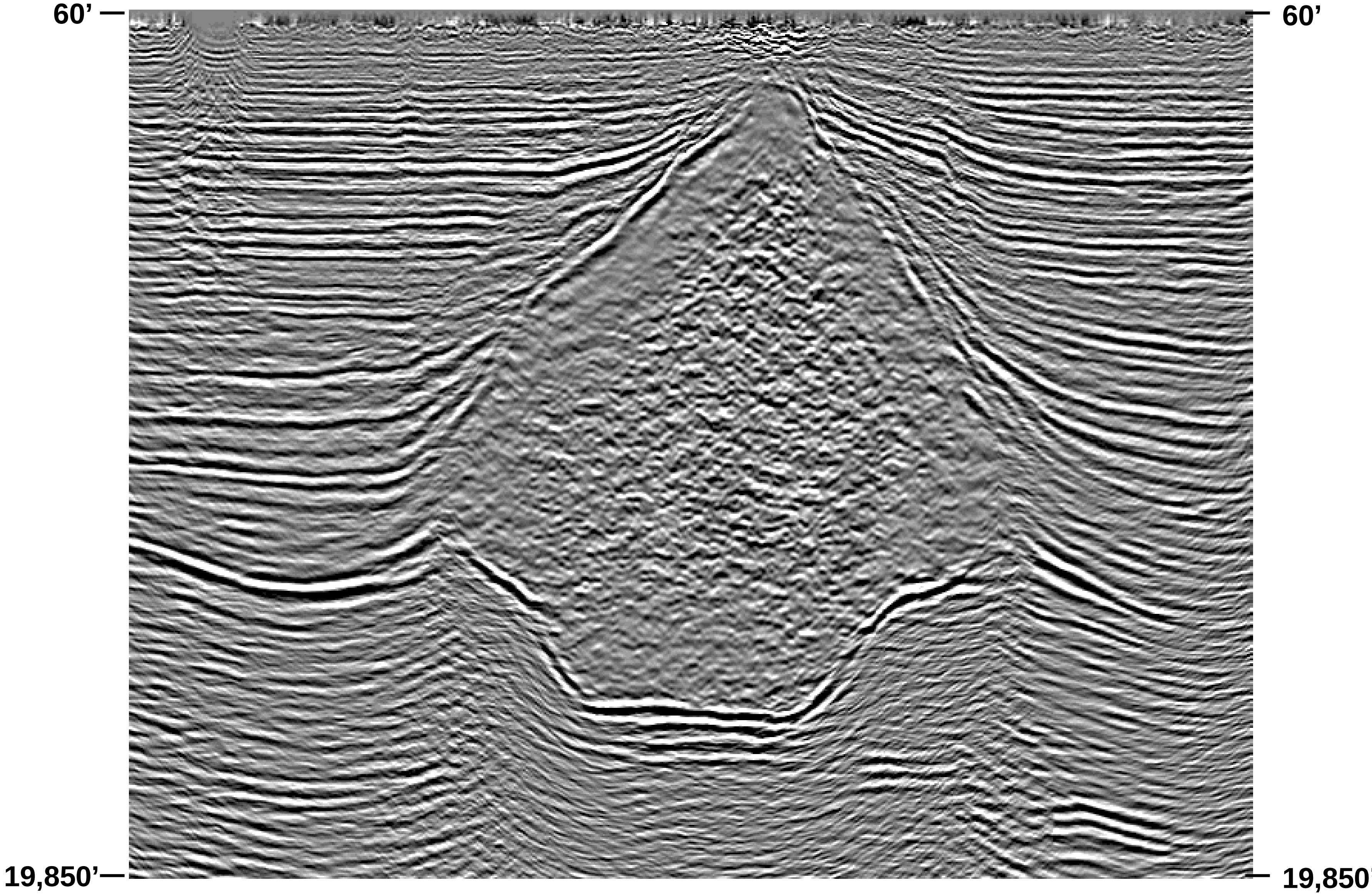

Figure 3.

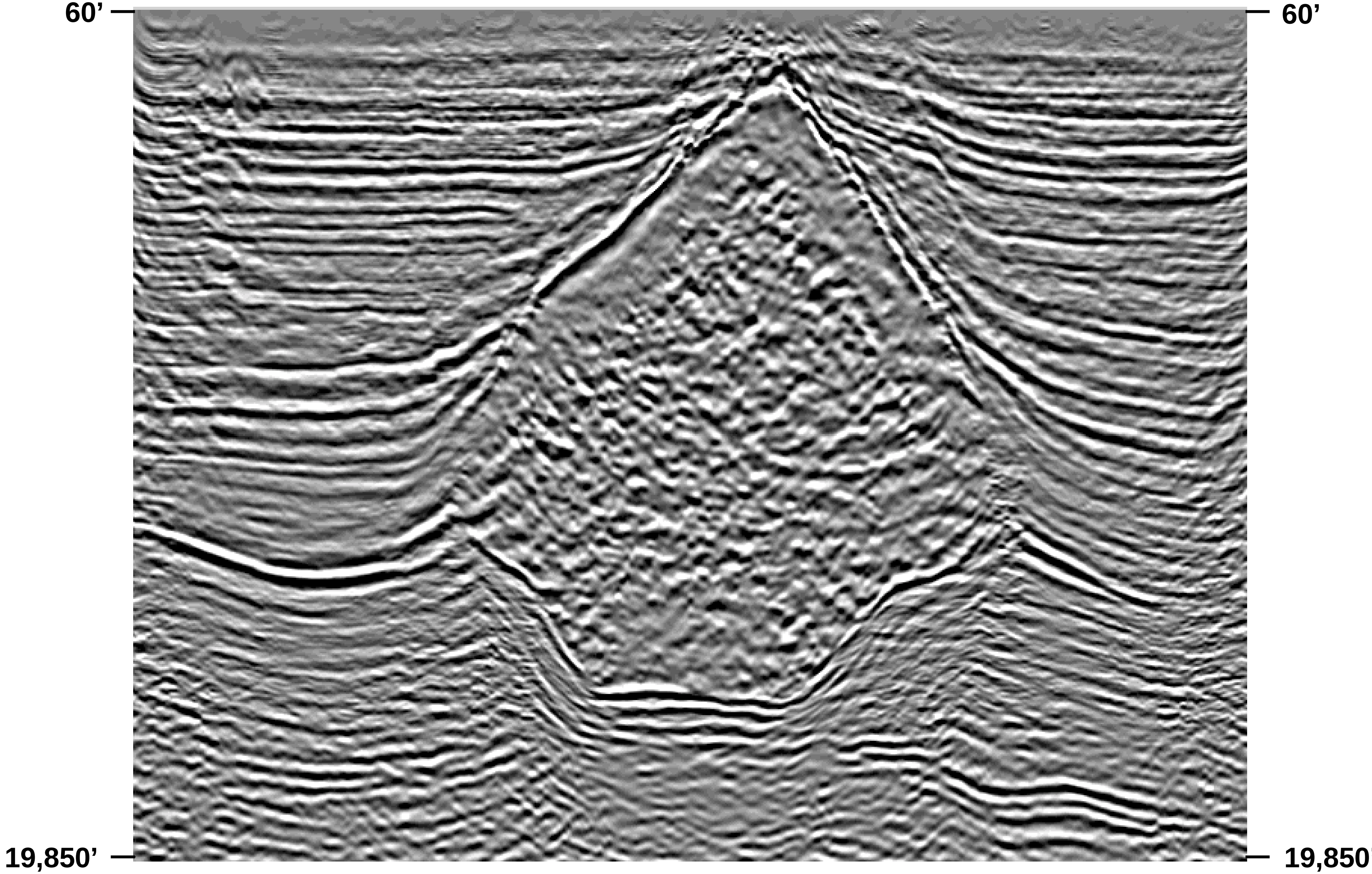

Figure 4

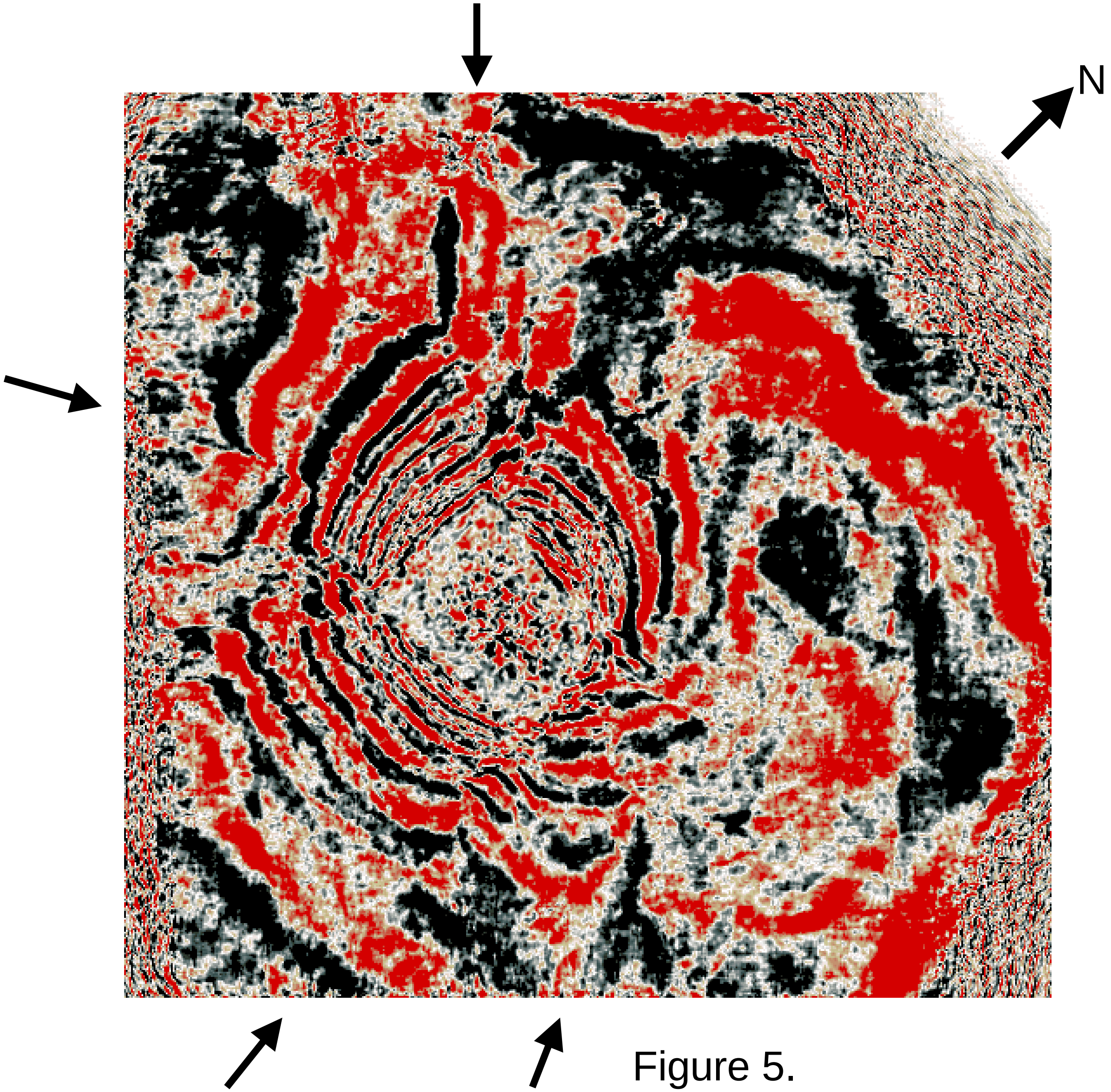

Figure 5.

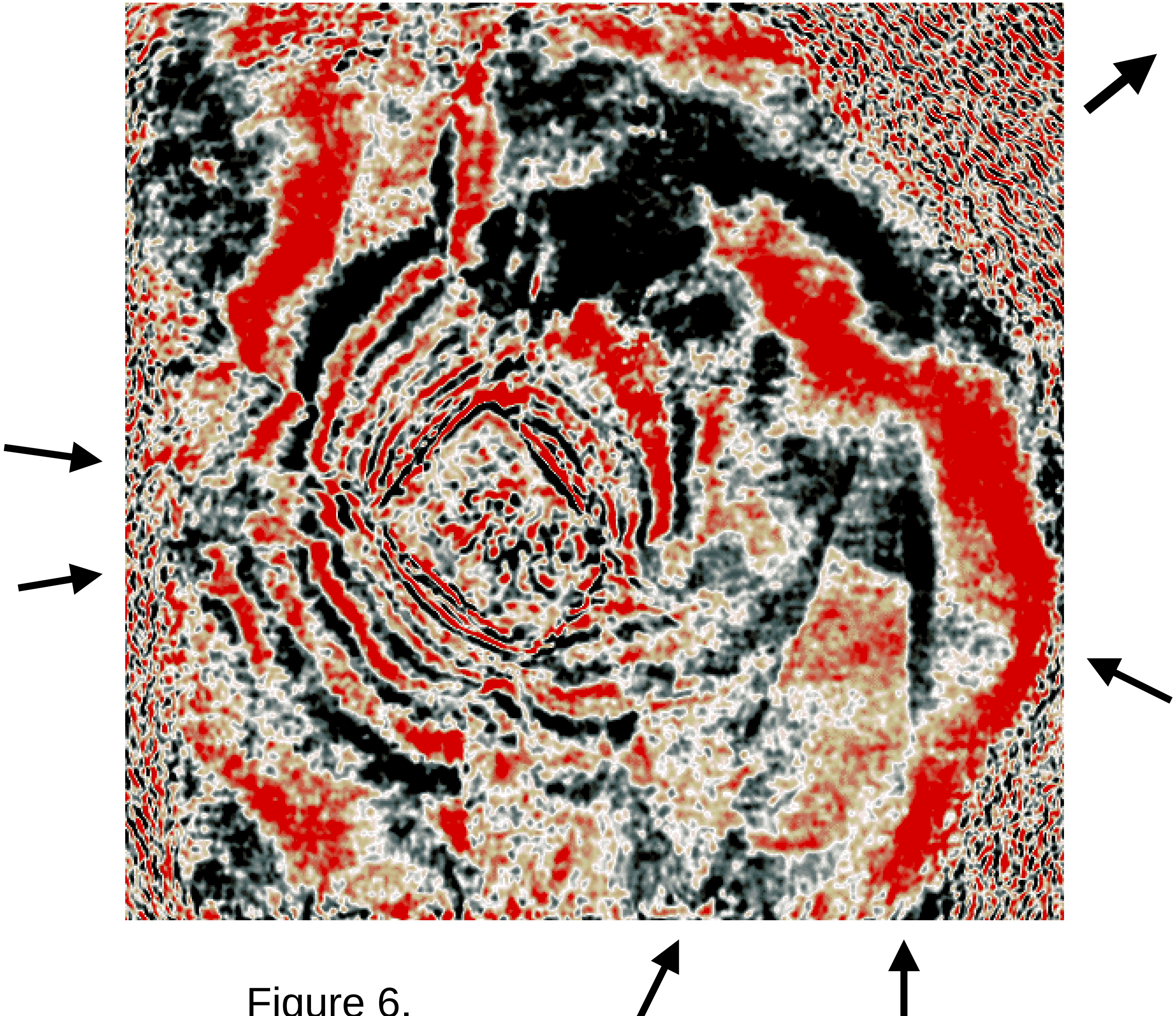

Figure 6.

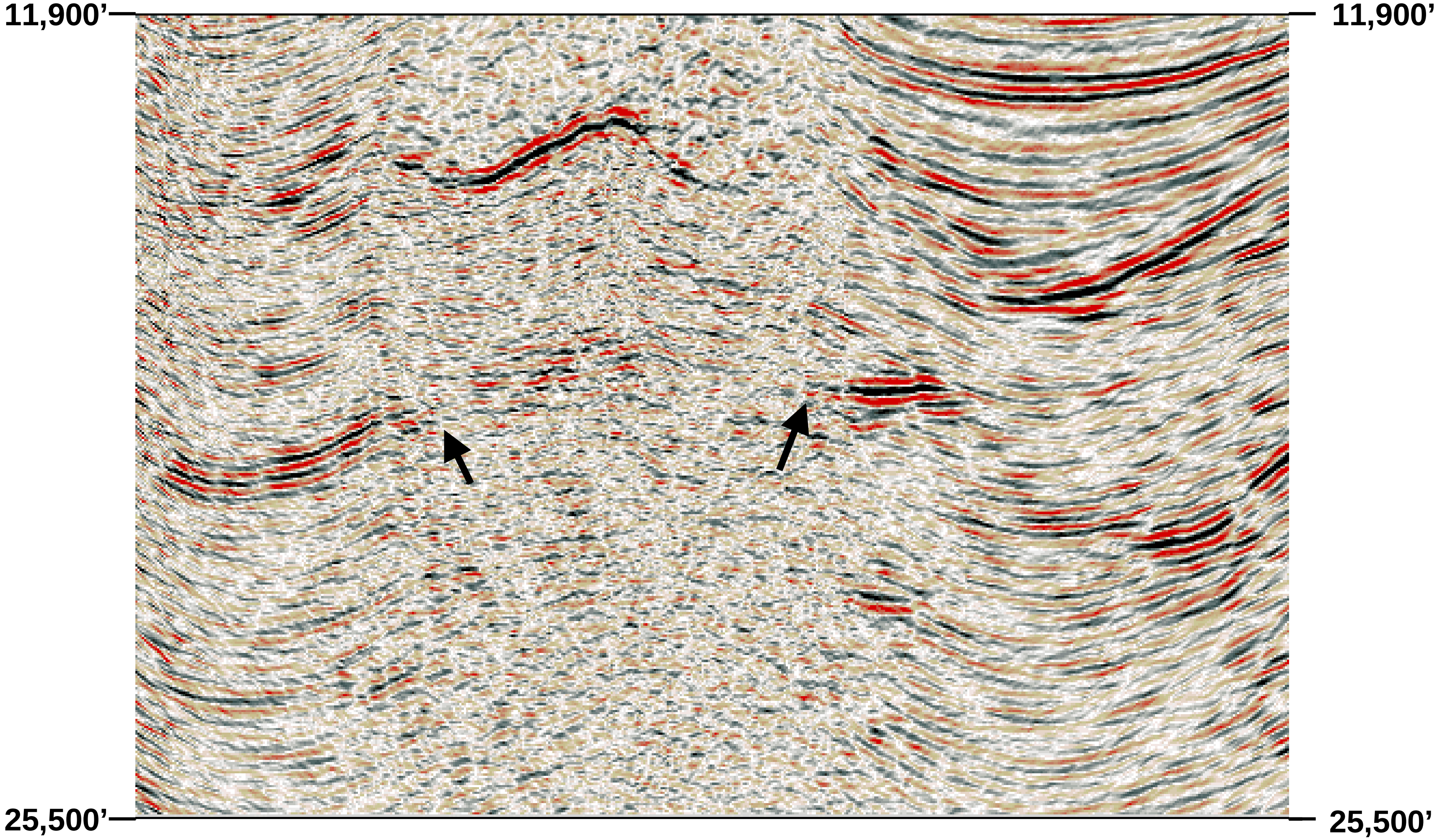

Figure 7.

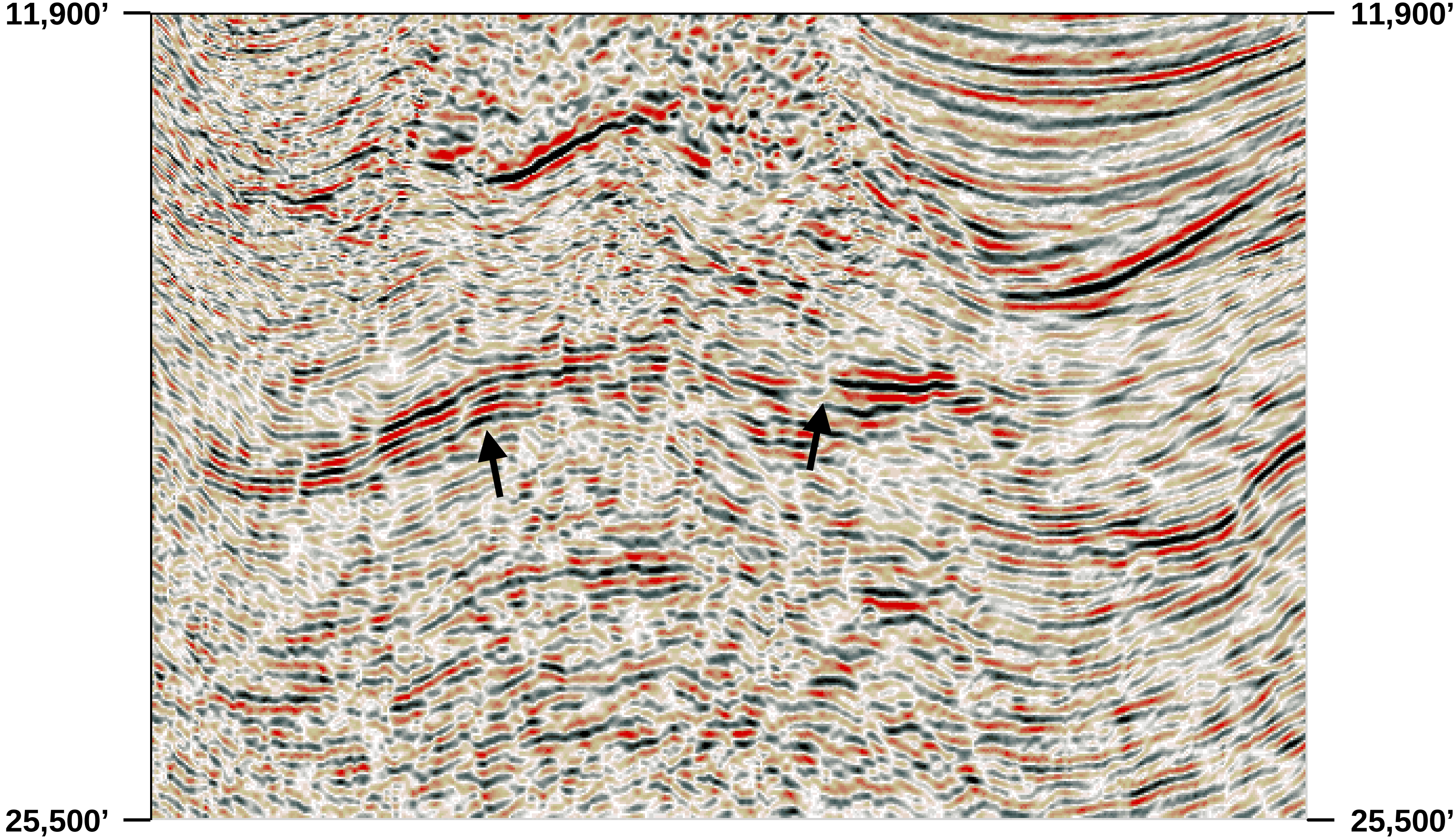

Figure 8.

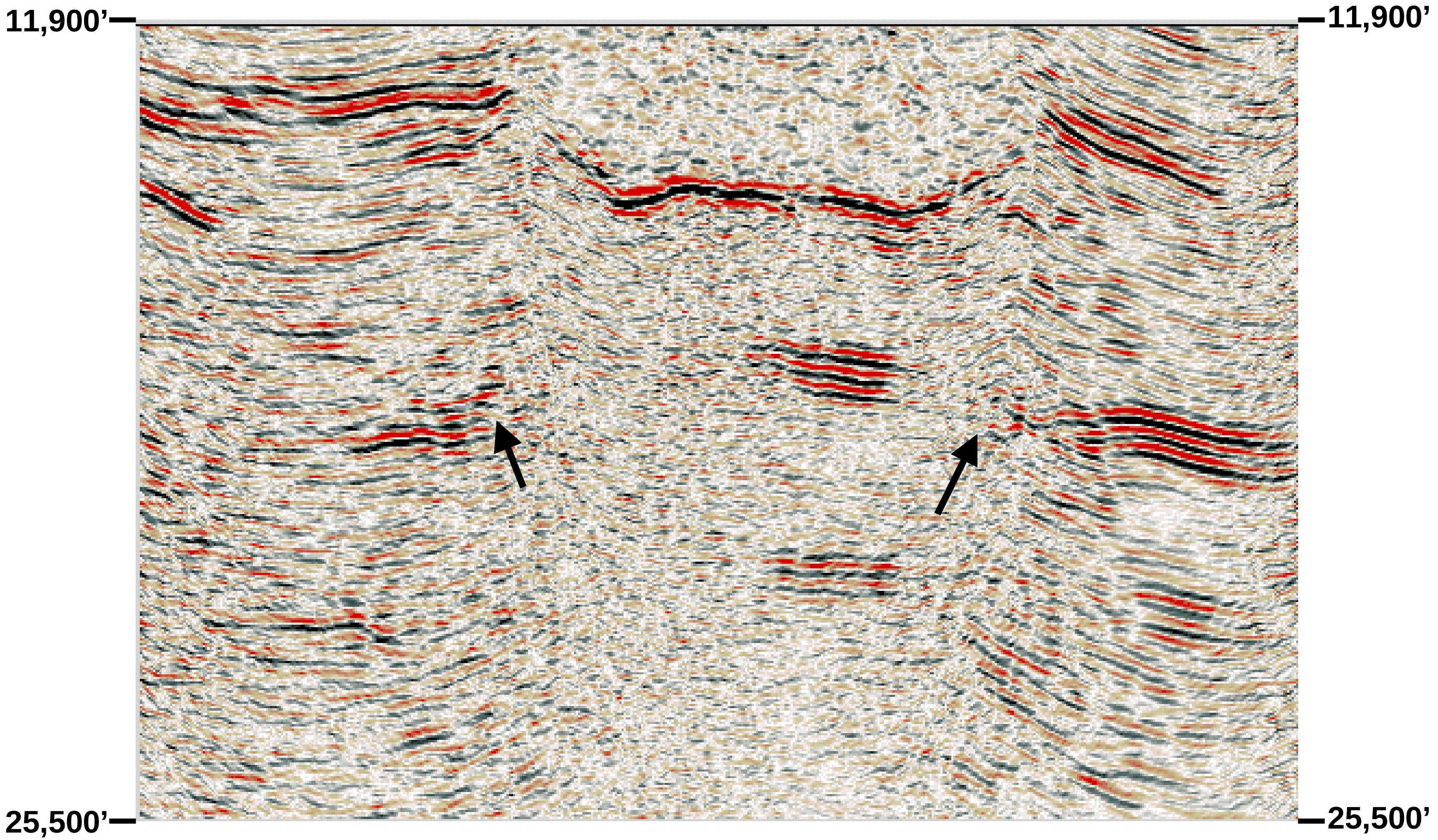

Figure 9.

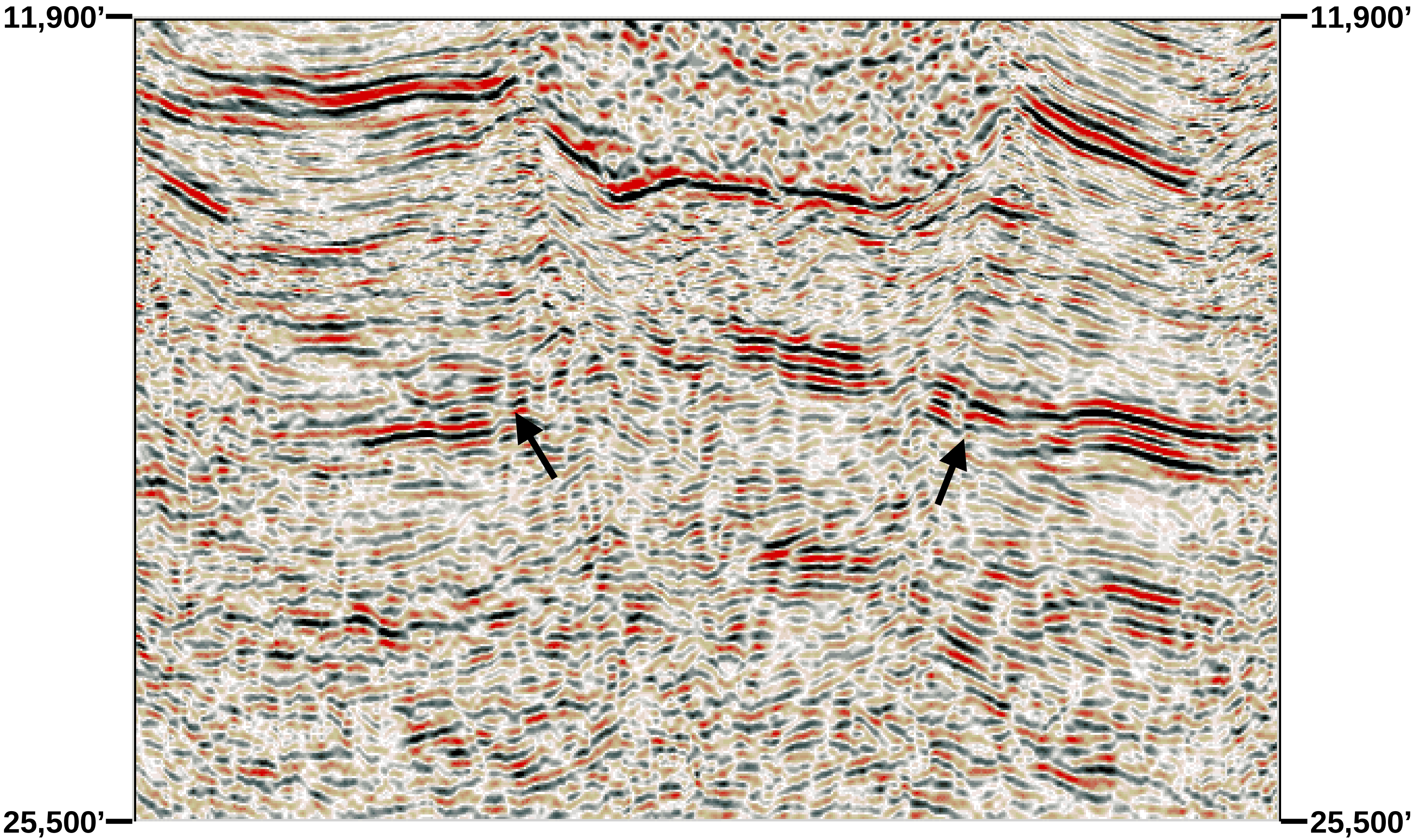

Figure 10.